



A novel electrochemical sensor for formaldehyde based on palladium nanowire arrays electrode in alkaline media

Yan Zhang^a, Min Zhang^b, Zhiquan Cai^b, Meiqiong Chen^b, Faliang Cheng^{b,*}

^a Department of Chemistry, Anhui University, Hefei 230039, China

^b Center of biosensor research, Dongguan University of Technology, Dongguan, Guangdong 523106, China

ARTICLE INFO

Article history:

Received 19 September 2011

Received in revised form 14 February 2012

Accepted 15 February 2012

Available online 25 February 2012

Keywords:

Pd nanowire (Pd NW) arrays

Formaldehyde

Sensor

ABSTRACT

A novel electrochemical sensor for the detection of formaldehyde based on palladium (Pd) nanowire (NW) arrays was developed. The Pd NW arrays were obtained via the direct electrodeposition of Pd on a glassy carbon electrode within the pores of an anodized aluminum oxide membrane. The electrocatalytic activity of the Pd NW arrays electrode for formaldehyde detection in alkaline media was then investigated via a series of electrochemical measurements; the results show the very high catalytic activity of the electrode. The formaldehyde oxidation on the Pd NW arrays electrode at +0.03 V, which is more negative than that in previous report. The experimental data further reveal that the electrooxidation of formaldehyde inhibits the formation of the poisonous intermediate, carbon monoxide. The proposed sensor has high sensitivity and fast response to formaldehyde, and the oxidation current has a linear relationship with the formaldehyde concentration in the 2 μ M to 1 mM range ($R = 0.9982$). The detection limit was 0.5 μ M ($S/N = 3$). The sensor has high sensitivity and good selectivity.

© 2012 Elsevier Ltd. All rights reserved.

1. Introduction

Formaldehyde is an important chemical widely applied in the manufacture of building materials and numerous household products [1–4]. It is found in foods (e.g., fruits, vegetables, and meat), beverages (e.g., beer and juices), and human biological fluids [5,6]. Recently, a new risk factor associated with formaldehyde and the process of ozonation has been revealed. Ozonation is a process used in potable water pretreatment involving the disinfection of water by removing iron and manganese, thereby eliminating unpleasant flavors and odors. Several kinds of toxic and mutagenic aldehydes (mostly formaldehyde) are generated as a result of the reaction of ozone with traces of humus [2,5].

Formaldehyde is found in more than 2000 products, to which many industrial workers are exposed on a daily basis. Chronic exposure to this chemical via ingestion leads to adverse gastrointestinal effects. Hence, the United States Environmental Protection Agency has set the daily intake of formaldehyde to 0.2 mg/kg body weight [6]. The International Agency for Research on Cancer has also classified formaldehyde as a human carcinogen [6]. These factors underscore the need for rapid, sensitive methods for the monitoring of trace concentrations of formaldehyde.

Various analytical methods that determine formaldehyde in air, food, water, and wood have been reported. The most common

methods include spectrophotometry [7], gas chromatography [8], high-performance liquid chromatography [9], and the use of sensors [2]. Compared with spectral and chromatographic analysis, sensors are low cost, simple, sensitive, and present operation. Sensors for the determination of formaldehyde concentration have been widely researched. Herschkovitz et al. [10] reported a novel formaldehyde detection method based on the coupling of a biosensor measuring device and a flow-injection system, using the enzyme formaldehyde dehydrogenase and a chemically modified Os(bpy)₂-poly(vinylpyridine) (POs-EA) screen-printed electrode. The as-produced sensor is low cost and has high selectivity, long-term stability, and simplicity of design and operation. Zhou et al. [13] introduced the electrodeposition of a nanostructured platinum–palladium (Pt–Pd) alloy in a Nafion film-coated glassy carbon electrode (GCE). The proposed alloy sensor not only possesses a broad linear range, good reproducibility, and high sensitivity, but also exhibits a synergistic effect that minimizes poison formation. Compared with biosensors, electrochemical sensors have a lower detection limit and a wider linear range. However, they have lower sensitivity and selectivity and a longer response time.

In recent years, electrochemical sensors have been widely applied in the determination of formaldehyde concentration [10–13]. Amperometric sensors in the potentiostatic mode using noble metals as electrode nanomaterials are also used for formaldehyde detection [3,14]. Metal nanomaterials have high effective surface areas and extraordinary electron-transport properties. Their use as electrochemical interfaces provides a rapid current

* Corresponding author. Fax: +86 769 22605545.

E-mail address: chengfl@dgut.edu.cn (F.L. Cheng).

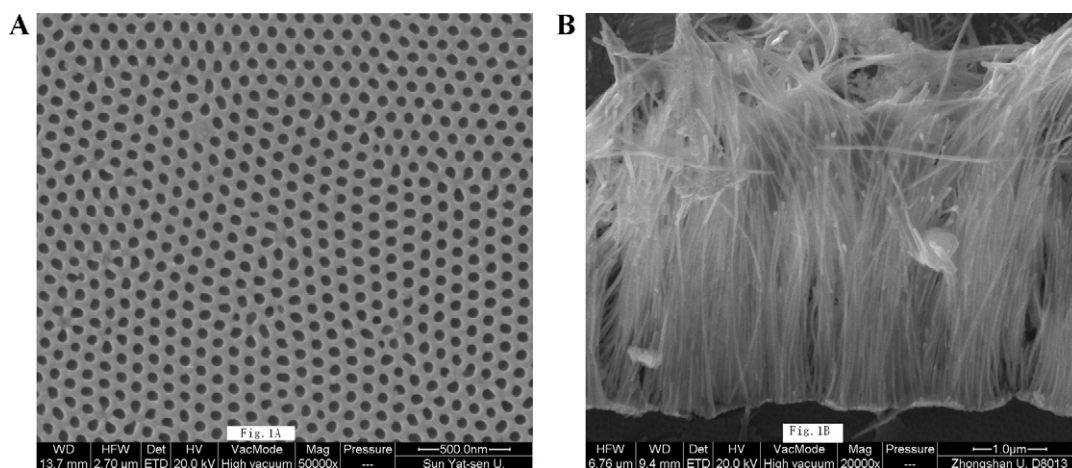


Fig. 1. (A) Typical SEM images of AAO template; (B) facet-section of Pd NW arrays.

response and high-detection sensitivity. Consequently, the electron transfer between the electrode and the probe molecules is accelerated [15].

Pt and Pd nanomaterials have high catalytic activities in the electrooxidation of small organic molecules. They are used as catalysts in many chemical reactions, such as alcohol oxidation reactions in fuel cells [16–18], electroanalytical processes [19,20], and sensor reactions [21–23]. The precious metal Pt [20,24,25] has been commonly used as the anode material in formaldehyde electrochemical sensors. However, poisonous chemisorbed species have been generated on Pt and Pt-based catalysts during the electrooxidation of formaldehyde. Pd is considered a substitute for Pt because of its equally high catalytic activity, lower cost, and reduced generation of poisonous substances [26,27].

Nanomaterials (nanoparticles, nanotubes, nanowires, and so on) are fabricated via a variety of preparative strategies [28–34]. The analytical applications of nanoparticles have been extensively explored for quite some time. However, studies related to the application of nanowires have been scarce. With the continuous advancements in nanotechnology, nanowires are attracting increased attention and interest because of their higher active surface areas compared with nanoparticles [35,36]. Therefore, the exploration of new applications for metal nanowires is a worthy endeavor. In the current paper, Pd nanowire (NW) arrays were prepared via anodized aluminum oxide (AAO) template electrodeposition. The as-prepared Pd NW arrays were used as enhanced electrochemical sensing electrodes for the measurement of formaldehyde. The experimental data reveal that the modified electrode has a very high catalytic activity for formaldehyde and effectively minimizes the formation of poisonous intermediates.

2. Experimental

2.1. Materials and reagents

High-purity aluminum foils (99.999%), formaldehyde (36–38%), acetone (99.5%), $\text{SnCl}_4 \cdot 5\text{H}_2\text{O}$, phosphoric acid (H_3PO_4 , 85%), and chromic trioxide (99%) were purchased from the Guangzhou Chemical Reagents Company (Guangzhou, China). $\text{K}_3\text{Fe}(\text{CN})_6$ and $\text{K}_4\text{Fe}(\text{CN})_6$ were obtained from Sigma–Aldrich (USA). $\text{Pd}(\text{NH}_3)_4\text{Cl}_2 + \text{NH}_4\text{Cl}$ was obtained from the Hong Kong Yuhua Noble Metal Chemical Engineering Electroplating Company (Hong Kong, China). All chemicals were analytical reagent grade, and all solutions were prepared using double-distilled water.

2.2. Apparatus

The electrochemical experiments were performed on a PAR-STAT 2273 electrochemical workstation (Princeton, USA) at 25 °C. A standard three-electrode system was used during the experiment. Pt and Ag/AgCl (saturated KCl) electrodes were used as the counter and reference electrodes, respectively. Scanning electron microscopy (SEM) analyses were performed using a Hitachi S-5200. Energy-dispersive X-ray spectroscopy (EDX) was conducted on an Oxford ISIS-300 EDX system.

2.3. Preparation of the AAO templates

Porous AAO templates were fabricated via a two-step anodization process in our laboratory [37,38]. Prior to anodization, high-purity aluminum foils (99.999%) were annealed in a vacuum at 500 °C for 4 h and were degreased in acetone. Anodization was performed in a 0.3 M H_2CO_4 solution for 2 h. The alumina layer was removed using a mixture of H_3PO_4 (6 wt%) and chromic acid (1.8 wt%). The aluminum foil was reoxidized under the same conditions for 6 h. The AAO template was etched in a saturated SnCl_4 solution to remove the remaining aluminum. The AAO template was again treated with 5 wt% H_3PO_4 at 25 °C for 30 min to remove the barrier layer on the other side of the aluminum foil.

2.4. Preparation of Pd NW arrays electrode

The Pd NW arrays were prepared via an AAO template electrodeposition method, as described in our previous work [23,39]. A GCE was polished and thoroughly cleaned, and a piece of the as-prepared AAO template was attached to the polished surface of the GCE. Electrodeposition was performed in an aqueous solution containing $\text{Pd}(\text{NH}_3)_4\text{Cl}_2 + \text{NH}_4\text{Cl}$. The pH value of the solution was adjusted to 8 using $\text{NH}_3 \cdot \text{H}_2\text{O}$. The Pd NW arrays electrode was prepared at -0.7 V, finally dipped in a 2 M NaOH solution for 1 h to completely remove the AAO, and washed with distilled water several times.

3. Results and discussion

3.1. Characterization

Fig. 1A shows a typical SEM image of the prepared AAO template, which exhibited pore arrays that were nearly aligned. The porous alumina structure consisted of cylindrical hexagonal cells with an

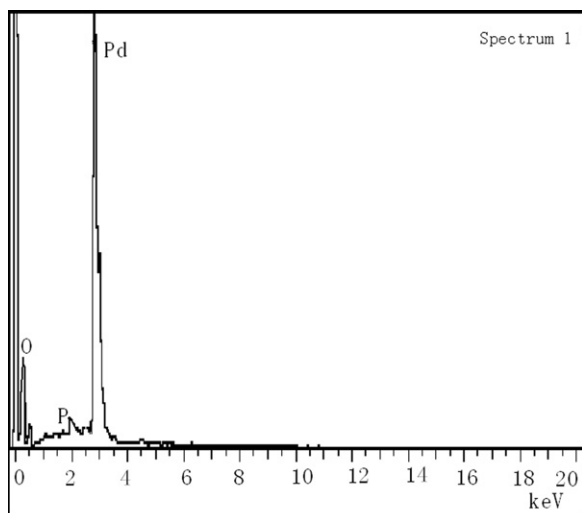


Fig. 2. Energy-dispersive X-ray spectroscopy (EDX) of Pd NW arrays.

average diameter of approximately 50 nm. The interface distance of each central pore was approximately 50 nm. Fig. 1B shows the typical SEM images of the Pd NW arrays, where the AAO template was completely dissolved. A large amount of Pd NW arrays was assembled in the AAO template. The straw shape of the Pd NW arrays exhibited a good orientation, which was perpendicular to the surface of the substrate. The diameters of the Pd NW arrays were approximately 50 nm, retaining the size and nearly cylindrical shape of the AAO template pores. Fig. 2 shows the EDX results of the Pd NW arrays. The major peaks correspond to Pd, showing that the AAO template was removed after treatment in the KOH solution and that the Pd NW arrays were indeed fabricated.

The impedance spectra of the bare GCE and the Pd NW arrays electrode in a 5 mM $\text{Fe}(\text{CN})_6^{3-/4-}$ + 0.1 M KCl solution are shown in Fig. 3(a) and (b), respectively; the frequency of the open-circuit potential varied from 0.1 Hz to 100 kHz. Electrochemical impedance spectroscopy (EIS) is an effective method of determining the interfacial properties of a modified electrode. It is often used to elucidate the chemical transformations and processes associated with conductive supports [40,41]. EIS curves consist of semicircular and linear parts. At high frequencies, the semicircular part corresponds to the electron-transfer limited process, and its diameter is equal to the electron-transfer resistance. This resistance controls the electron-transfer kinetics of the redox probe at the electrode interface [41,42]. In the present study, the Pd NW arrays electrode

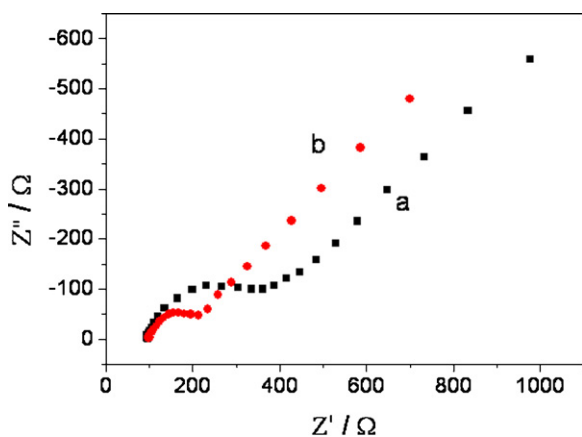


Fig. 3. EIS of bare GCE (a) and Pd NW arrays electrode (b) in a 0.1 M KCl containing 5 mM $\text{Fe}(\text{CN})_6^{3-/4-}$. Applied frequency was from 0.1 Hz to 100 kHz.

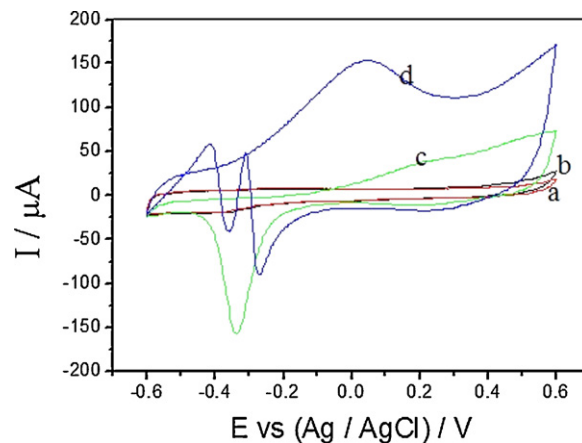


Fig. 4. CVs of 5 mM formaldehyde in 0.1 M KOH solution at bare electrode in the absence and presence of formaldehyde (a and b), respectively; at Pd NW arrays electrode in the absence and presence of formaldehyde (c and d), respectively. Scan rate: 100 mV/s.

clearly had a lower electron-transfer resistance than the bare GCE, implying that the Pd NW arrays play an important role in providing the conducting bridges for the charge transfer of $\text{Fe}(\text{CN})_6^{3-/4-}$.

3.2. Electrochemistry of the sensor

The cyclic voltammetry (CV) curves of formaldehyde oxidation on the bare GCE and the Pd NW arrays electrode are shown in Fig. 4. Fig. 4(a) and (c) show the CV of the bare and Pd NW arrays electrode in a 0.1 M KOH solution. The background current on the Pd NW arrays electrode (Fig. 4(c)) was much higher than that on the bare electrode, probably because of the larger surface area of the Pd NW arrays electrode [26,43]. Pd oxides were generated for the positive scan, and a sharp reduction in the current peak at approximately -0.35 V for the reverse scan was due to the reduction of the Pd oxides formed during the positive potential sweep.

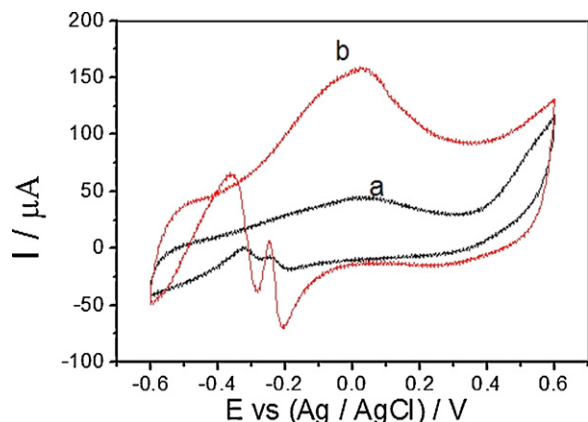
After the addition of 5 mM formaldehyde to the 0.1 M KOH solution, no current peak appeared for the bare GCE (Fig. 4(b)). This finding indicates that the bare GCE had no electrocatalytic activity toward formaldehyde oxidation. The CV curve of formaldehyde oxidation on the Pd NW arrays electrode is shown in Fig. 4(d). The oxidation was characterized by two well-defined current peaks on the positive and reverse scans. An oxidation peak observed at approximately $+0.05$ V corresponds to the oxidation of formaldehyde on the Pd NW arrays electrode. Another oxidation current peak found at approximately -0.3 V is ascribed to the further anodic oxidation of the intermediates formed during the positive potential scan. Compared with previous reports (Table 1), the peak potential ($+0.05$ V) for the oxidation of formaldehyde in the current study is much lower, indicating that the sensor has superior electrocatalytic activity for formaldehyde.

The CV curves for formaldehyde oxidation on the Pd nanoparticle-modified and Pd NW arrays electrode are shown in Fig. 5(a) and (b), respectively. The oxidation peak current was $45 \mu\text{A}$ at $+0.05$ V on the Pd nanoparticle-modified electrode and $157 \mu\text{A}$ at $+0.05$ V on the Pd NW arrays electrode. The oxidation current on the NW arrays electrode is three times higher than that on the nanoparticle-modified electrode, indicating that the Pd NW arrays electrode have higher activity than the nanoparticle-modified one for formaldehyde oxidation in alkaline media. A similar report for the comparison of the oxidation peak currents on Pd nanoparticles and Pd nanowires was found for the oxidation of formic acid [45]. In the current work, the superior activity may be related to the fast electronic conduction and good orientation of the perpendicular array structure.

Table 1

Comparison of the working potential, linear range, detection limit, correlation coefficient of our sensor with other electrochemical sensors from the previous methods.

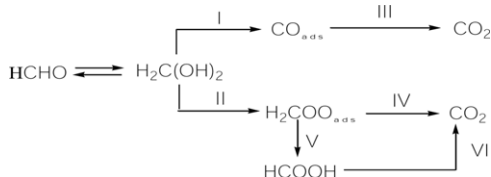
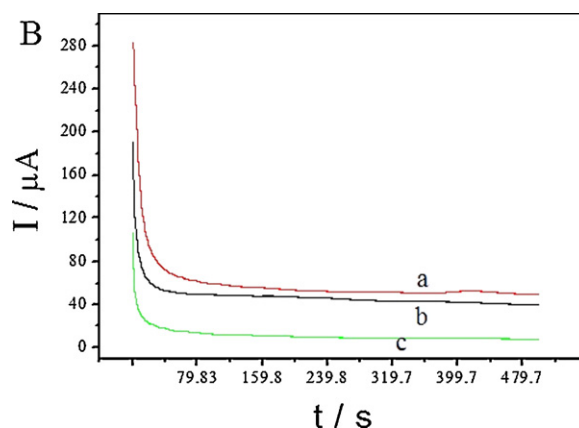
Electrode fabrication	Detection potential	Linearity range	Detection limit	R	Ref.
Pd NP/CILE/GCE	0.15 V	20–100 mM	–		[26]
Pt-SnO ₂ /sol-gel/GCE	0.6 V				[44]
Pd NP/TiO ₂ /GCE	-0.4 V	0–17.7 mM	15 μM		[43]
Pt-Pd NP/Nafion/GCE	0.57 V	10 μM to 1 mM	3 μM	0.9983	[13]
Pt NP/PANI/MWNCs/GCE	0.3 V	1 ppm to 1 mM	0.046 ppm	0.999	[24]
Pd NW/GCE	0.05 V	2 μM to 1 mM	0.5 μM	0.9982	Our work

**Fig. 5.** CVs of 5 mM formaldehyde in 0.1 M KOH solution at Pd nanoparticle-modified electrode (a) and Pd NW arrays electrode (b). Scan rate: 100 mV/s.

The oxidation mechanism of small organic molecules on Pt-Pd-based catalysts follows a dual pathway [46–49]. According to Safavi et al. [26], formaldehyde is oxidized to CO₂ via two parallel pathways (Scheme 1). One is the indirect electrooxidation of formaldehyde via the formation of a chemisorbed CO intermediate, whereas the other is a direct electrooxidation via the formation of active adsorbed intermediates. The presence of oxidation peaks in the forward and reverse scans indicates that formaldehyde oxidation followed a dual pathway. The poisonous intermediate CO_{ads} requires a higher electrode potential to be further oxidized into CO₂. However, the oxidation of formaldehyde on the Pd NW arrays electrode had a lower potential. Hence, the electrochemical oxidation of formaldehyde probably occurred mainly via the direct pathway.

Chronoamperometry was used to further examine the electrocatalytic activity of the formaldehyde sensor at different electrode potentials (Fig. 6). Fig. 4 shows that the oxidation of formaldehyde on the Pd NW arrays electrode occurred at low potential regions. Therefore, the applied potentials of +0.05, 0.00, and +0.30 V (Fig. 6(a)–(c)) were chosen for the determination of the formaldehyde concentration. We can see that the current decays quickly to a steady-state value. The oxidation current at +0.05 V was the highest compared with those at 0.00 and +0.30 V. Hence, the operating potential of +0.03 V was chosen for the formaldehyde sensor.

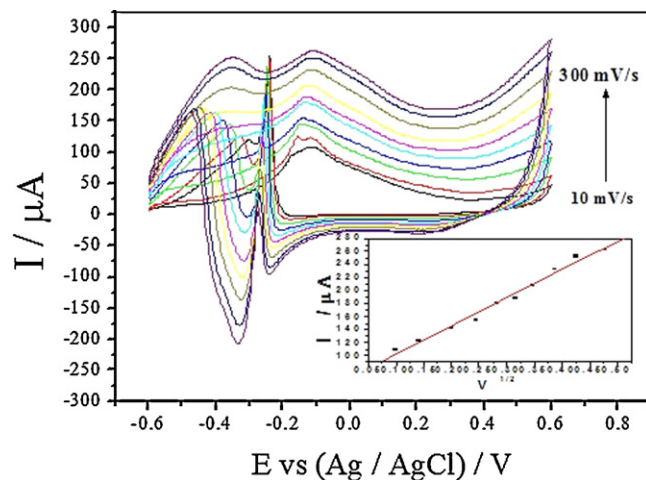
The kinetics of formaldehyde oxidation was also investigated. Fig. 7 shows the CVs of the proposed sensor in the 5 mM formaldehyde + 0.1 M KOH solution. The scan rate was increased from 10 mV/s to 300 mV/s. The anodic peak current for the positive

**Scheme 1.** Schematic representation of formaldehyde oxidation.**Fig. 6.** Chronoamperometry of the Pd NW arrays electrode in a solution of 5 mM HCHO + 0.1 M KOH. The electrode potentials were +0.05 V (a), 0.00 V (b) and +0.3 V (c), respectively.

scan was linearly proportional to the square root of the scan rate ($R=0.9934$), indicating that the electrode process was controlled via diffusion.

3.3. Amperometric detection of formaldehyde

The typical current–time plot of the sensor with successive injection of 0.01 M formaldehyde is given in Fig. 8A. The working potential was set at +0.05 V, where the amperometric response reached the maximum value (Fig. 4). The sensor rapidly responded and reached a steady state within 5 s after the formaldehyde was added into solution (as insert in Fig. 8A), demonstrating that the sensor had a high sensitivity to formaldehyde. The fast response time and high sensitivity can also be ascribed to the well-defined

**Fig. 7.** CVs of 5 mM formaldehyde in 0.1 M KOH solution on the Pd NW arrays electrode with different scan rates: 10, 20, 40, 60, 80, 100, 150, 200, 250, 300 mV/s (inset: the relation of the anodic peak current for the positive scan with square root of scan rate).

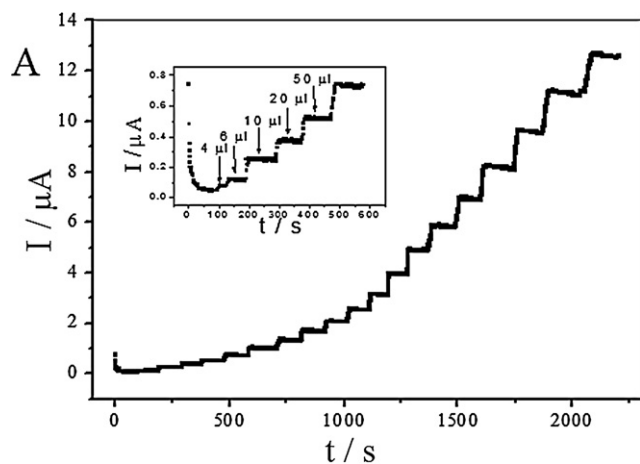


Fig. 8. (A) Current–time response of the electrochemical sensor for successive addition of 0.01 M formaldehyde in N_2 -saturated 0.1 M KOH. The applied potential is +0.05 V (inset: amplification of part with low formaldehyde concentrations). (B) Calibration curve of steady-state current vs. the concentration of formaldehyde in N_2 -saturated 0.1 M KOH. The applied potential is +0.05 V.

surface area. Fig. 8B shows the calibration curve of the amperometric response. A good linear relationship was realized within the formaldehyde concentration range of 2 μ M to 1 mM, with a correlation coefficient of 0.9982. The detection limit for formaldehyde was estimated at 0.5 μ M, at a signal-to-noise ratio of 3.

The analytical performance of the prepared sensor was compared with those of other chemosensors (Table 1) and biosensors (Table 2). Through comparison and analysis, we the proposed sensor was shown to exhibit good performance in terms of a low oxidation potential, a wide linear range, and good sensitivity, which may be the result of the fast electronic conduction and good orientation of the perpendicular arrays structure.

3.4. Sensor selectivity

Interferences from electroactive compounds such as acetaldehyde, ethanol, and 1-propanol, among others, can cause problems in the accurate determination of formaldehyde. The CVs for the Pd NW arrays electrode in the presence of 5 mM formaldehyde, 5 mM acetaldehyde, 5 mM ethanol, and 5 mM 1-propanol are shown in Fig. 9(a)–(d), respectively. The sharp current peak at approximately +0.05 V in Fig. 9(a) corresponds to the oxidation current peak of formaldehyde. The selectivity of the formaldehyde sensor against

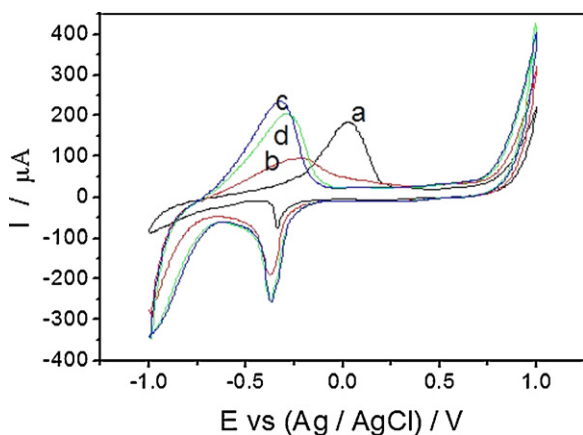


Fig. 9. CVs for Pd NW arrays electrode in (a) 5 mM formaldehyde+0.1 M KOH, (b) 5 mM acetaldehyde+0.1 M KOH, (c) 5 mM ethanol+0.1 M KOH and (d) 5 mM 1-propanol+0.1 M KOH. Scan rate: 100 mV/s.

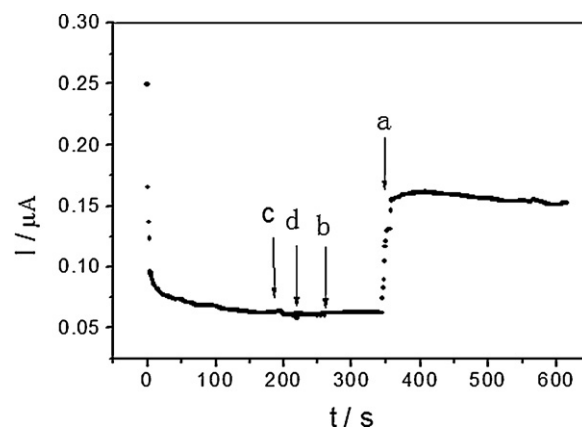


Fig. 10. Amperometric response of Pd NW arrays electrode to (a) 5 mM formaldehyde, (b) 5 mM acetaldehyde, (c) 5 mM ethanol and (d) 5 mM 1-propanol in 0.1 M KOH solution. The applied potential is +0.05 V.

the interfering species was investigated by measuring the amperometric response to the successive addition the same volume of 5 mM formaldehyde (a), 5 mM acetaldehyde (b), 5 mM ethanol (c), and 5 mM 1-propanol (d) at the +0.05 V potential (Fig. 10). No obvious current changes were observed when acetaldehyde, ethanol, and 1-propanol were added. However, a fast current response occurred after the addition of formaldehyde. These results indicate that acetaldehyde, ethanol, and 1-propanol showed almost no interference to formaldehyde detection.

3.5. Reproducibility and stability of the sensor

The relative standard deviation (RSD) of the sensor response to 5 mM formaldehyde was 1.1% for 20 successive measurements, indicating good repeatability. The reproducibility was evaluated from the response of 10 electrodes fabricated under the same conditions to 5 mM formaldehyde. The RSD obtained was 7.8%.

Long-term stability is an important parameter in evaluating the performance of a sensor. The stability of the formaldehyde sensor was determined using CV by measuring the decrease in the voltammetric peak current during potential cycling. The response of the electrodes to 30 cycles in the potential range of -0.7 to 0.7 V is shown in Fig. 11. The peaks on the first scans are higher than those on the subsequent scans. However, starting from the third scan, the catalytic activity of the Pd NW arrays electrode only slightly varied. The catalytic current was reduced to 80.15% after 30 tests. The electrode was kept at 4 $^{\circ}$ C in a refrigerator. Afterward, the catalytic

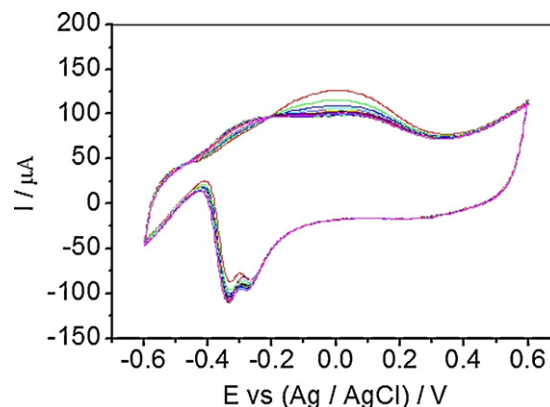


Fig. 11. CVs of formaldehyde oxidation on the Pd NW arrays electrode in 0.1 M KOH solution containing 5 mM formaldehyde. Scan rate: 100 mV/s.

Table 2

Comparison of the linear range, detection limit, sensitivity of our sensor with other biosensors from the previous methods.

	Linearity range	Detection limit	Sensitivity	Ref.
Bio-functionalized Si/SiO ₂ /Si ₃ N ₄	10 μM to 25 mM	10 μM	31 mA M ⁻¹ cm ⁻²	[2]
FDH-ECH-Sepharose (in solution)	10 μM to 0.1 mM	5 μM	0.24 μS/μM	[50]
FDH-ECH-Sepharose (in air)	0.05–2 ppm	50 ppb	20 μS/ppm	[50]
Pd NW/GCE	2 μM to 1 mM	0.5 μM	1.36 mA M ⁻¹ cm ⁻²	Our work

current retained 90.7% of the initial value after 7 d. The signal current also retained more than 85% of its initial value after 2 months. The decreased current values may be attributed to the generation of poisonous organic compounds as well as to the consumption of formaldehyde.

4. Conclusions

Pd NW arrays were successfully prepared via a template-synthesis method by direct electrodeposition. The procedure represents a promising route for the synthesis of other materials with well-defined structures. Compared with Pd nanoparticles, the Pd NW arrays exhibited a higher catalytic activity for formaldehyde detection. The mechanism of formaldehyde oxidation on the Pd NW arrays electrode was also investigated. The result shows that the fabricated sensor can effectively minimize the formation of poisonous intermediates. Furthermore, the fabricated formaldehyde sensor effectively detected formaldehyde in the presence of interferences such as acetaldehyde, ethanol, and 1-propanol. Overall, the sensor has potential applications in practical analyses.

Acknowledgments

This work was supported by the National Natural Science Foundation of China (No. 20975020), the Natural Science Foundations of Guangdong Province (No. 10151170003000000), Technology Project of Guangdong Province (No. 2009B030802001) and Technology Project of Dongguan (No. 201010824000005).

References

- [1] S. Achmann, M. Hmmerle, R. Moos, *Electroanalysis* 20 (2008) 410.
- [2] M.B. Ali, M. Gonchar, G. Gayda, S. Paryzhak, M.A. Maaref, N. Jaffrezic-Renault, Y. Korpan, *Biosens. Bioelectron.* 22 (2007) 2790.
- [3] R. Knake, P. Jacquinet, P.C. Hauser, *Electroanalysis* 13 (2001) 631.
- [4] A.A. Mohamed, A.T. Mubarak, Z.M.H. Marestani, K.F. Fawy, *Talanta* 74 (2008) 578.
- [5] Y.I. Korpan, M.V. Gonchar, A.A. Sibirny, C. Martelet, A.V. El'skaya, T.D. Gibson, A.P. Soldatkin, *Biosens. Bioelectron.* 15 (2000) 77.
- [6] X.Q. Zhao, Z.Q. Zhang, *Talanta* 80 (2009) 242.
- [7] L.S.G. Teixeira, E.S. Leão, A.F. Dantas, H.L.C. Pinheiro, A.C.S. Costa, J.B. de Andrade, *Talanta* 64 (2004) 711.
- [8] F. Bianchi, M. Careri, M. Musci, A. Mangia, *Food Chem.* 100 (2007) 1049.
- [9] J.J. Michels, *J. Chromatogr. A* 914 (2001) 123.
- [10] Y. Herschkovitz, I. Eshkenazi, C.E. Campbell, J. Rishpon, *J. Electroanal. Chem.* 491 (2000) 182.
- [11] W. Sun, G. Sun, B. Qin, Q. Xin, *Sens. Actuators B* 128 (2007) 193.
- [12] J. Wang, P. Zhang, J.Q. Qi, P.J. Yao, *Sens. Actuators B* 136 (2009) 399.
- [13] Z.L. Zhou, T.F. Kang, L. Zhang, S.Y. Cheng, *Microchim. Acta* 164 (2009) 133.
- [14] R. Knake, R. Guchardi, P.C. Hauser, *Anal. Chim. Acta* 475 (2003) 17.
- [15] D. Wen, S. Guo, S. Dong, E.K. Wang, *Biosens. Bioelectron.* 26 (2010) 1056.
- [16] C. Bianchini, P.K. Shen, *Chem. Rev.* 109 (2009) 4183.
- [17] J.P. Liu, J.Q. Ye, C.W. Xu, S.P. Jiang, Y.X. Tong, *J. Power Sources* 177 (2008) 67.
- [18] P.K. Shen, C.W. Xu, *Chem. Commun.* 8 (2006) 184.
- [19] Q.F. Yi, W. Huang, X.Q. Liu, G.R. Xu, Z.H. Zhou, A.C. Chen, *J. Electroanal. Chem.* 15 (2008) 197.
- [20] S. Park, Y. Xie, M.J. Weaver, *Langmuir* 18 (2002) 5792.
- [21] Z.P. Li, J.F. Li, X. Wu, S.M. Shuang, S.M. Dong, M.M.F. Choi, *Sens. Actuators B* 139 (2009) 453.
- [22] K. Mitsubayashi, G. Nishio, M. Sawai, T. Saito, H. Kudo, H. Saito, K. Otsuka, T. Noguer, J.L. Marty, *Sens. Actuators B* 130 (2008) 32.
- [23] M. Zhang, F.L. Cheng, Z.Q. Cai, H.J. Yao, *Int. J. Electrochem. Sci.* 5 (2010) 1026.
- [24] G.P. Jin, J. Li, X. Peng, *J. Appl. Electrochem.* 39 (2009) 1889.
- [25] Z. Wang, Z.Z. Zhu, J. Shi, H.L. Li, *Appl. Surf. Sci.* 153 (2007) 8811.
- [26] A. Safavi, N. Maleki, F. Farjami, E. Farjami, *J. Electroanal. Chem.* 626 (2009) 75.
- [27] J.P. Wang, P. Holt-Hindle, D. MacDonald, D.F. Thomas, A. Chen, *Electrochim. Acta* 53 (2008) 6944.
- [28] P.H.C. Camargo, Y.J. Xiong, L. Ji, J.M. Zuo, Y.N. Xia, *J. Am. Chem. Soc.* 129 (2007) 15452.
- [29] X. Cao, N. Wang, L. Wang, C. Mo, Y.J. Xu, X.L. Cai, G. Lin, *Sens. Actuators B* 147 (2010) 730.
- [30] X. Che, R. Yuan, Y.Q. Chai, J.J. Li, Z.J. Song, W.J. Li, *Electrochim. Acta* 55 (2010) 5420.
- [31] X.M. Chen, Z.J. Lin, D.J. Chen, T.T. Jia, Z.M. Cai, X.R. Wang, X. Chen, G.N. Chen, M. Oyama, *Biosens. Bioelectron.* 25 (2010) 1803.
- [32] S. Cherevko, C.H. Chung, *Sens. Actuators B* 142 (2009) 216.
- [33] V. Selvaraj, A.N. Grace, M. Alagar, *J. Colloid Interface Sci.* 333 (2009) 254.
- [34] V.S. Tripathi, V.B. Kandimalla, H.X. Ju, *Biosens. Bioelectron.* 21 (2006) 1529.
- [35] S.M. Choi, J.H. Kim, J.Y. Jung, E.Y. Yoon, W.B. Kim, *Electrochim. Acta* 53 (2008) 5804.
- [36] Z.X. Liang, T.S. Zhao, *J. Phys. Chem. C* 111 (2007) 8128.
- [37] H. Wang, C.W. Xu, F.L. Cheng, S.P. Jiang, *Electrochem. Commun.* 9 (2007) 1212.
- [38] C.W. Xu, H. Wang, P.K. Shen, S.P. Jiang, *Adv. Mater.* 17 (2007) 4256.
- [39] F.L. Cheng, H. Wang, Z.H. Sun, M.X. Ning, Z.Q. Cai, M. Zhang, *Electrochem. Commun.* 10 (2008) 798.
- [40] E. Katz, I. Willner, *Electroanalysis* 15 (2003) 913.
- [41] L.Q. Luo, Q.X. Li, Y.H. Xu, Y.P. Ding, X. Wang, D.M. Deng, Y.J. Xu, *Sens. Actuators B* 145 (2010) 293.
- [42] Q.L. Sheng, Y. Shen, H.F. Zhang, J.B. Zheng, *Chin. J. Chem.* 26 (2008) 1244.
- [43] Q.F. Yi, F.J. Niu, W.Q. Yu, *Thin Solid Films* 519 (2011) 3155.
- [44] H.M. Villullas, F.I. Mattos-Costa, P.A.P. Nascente, L.O.S. Bulhões, *Electrochim. Acta* 49 (2004) 3909.
- [45] J.J. Wang, Y.G. Chen, H. Liu, R.Y. Li, X.L. Sun, *Electrochem. Commun.* 12 (2010) 219.
- [46] S. Ivanov, U. Lange, V. Tsakova, V.M. Mirsky, *Sens. Actuators B* 150 (2010) 271.
- [47] T. Iwasita, X.H. Xia, H.D. Liess, W. Vielstich, *J. Phys. Chem. B* 101 (1997) 7542.
- [48] Z.J. Li, Z.R. Zhang, B.D. Kay, Z. Dohnalek, *J. Phys. Chem. C* 115 (2011) 9692.
- [49] H. Wang, C.W. Xu, F.L. Cheng, M. Zhang, S.Y. Wang, S.P. Jiang, *Electrochem. Commun.* 10 (2008) 1575.
- [50] F. Vianello, R. Boscolo-Chio, S. Signorini, A. Rigo, *Biosens. Bioelectron.* 22 (2007) 920.